

# Crystallisation Behaviour and Polytype Transformation of Polymer-Derived Silicon Carbide

Hans-Peter Martin,<sup>a</sup> Eberhard Müller,<sup>a</sup> Gert Irmer<sup>b</sup> & Florence Babonneau<sup>c</sup>

<sup>a</sup>TU Bergakademie Freiberg, Institut für Keramische Werkstoffe, Zennerstr. 3, 09596 Freiberg, Germany

<sup>b</sup>Institut für Theoretische Physik, Freiberg, Cottastr. 4, 09596 Freiberg, Germany

<sup>c</sup>Université Pierre et Marie Curie, Chimie de la Matière Condensée, 4 Place Jussieu, 75252 Paris, Cedex 05 France

(Received 28 February 1996; accepted 21 May 1996)

## Abstract

*This paper describes the crystallisation behaviour of polysilane-derived amorphous silicon carbide. The polytype formation and the transformation from  $\beta$ -SiC into hexagonal  $\alpha$ -polytypes have been more specifically investigated by X-ray diffraction (XRD), transmission electron microscopy (TEM), <sup>29</sup>Si Solid State Magic Angle Spinning Nuclear Magnetic Resonance (<sup>29</sup>Si MAS-NMR) and Raman spectroscopy. The crystallisation of  $\beta$ -SiC starts around 1200°C. The different polytypes like 3C, 2H, 4H, 6H and 15R have been identified by the various investigation techniques at temperatures higher than 1400°C. Crystallisation occurs with a high density of stacking faults that cover large areas in the crystallites as found by TEM observation. They promote the formation of temporary existing  $\alpha$ -polytypes which are finally reconverted into  $\beta$ -SiC as found by X-ray and electron diffraction. © 1997 Elsevier Science Limited. All rights reserved.*

## Introduction

The polymeric route to silicon carbide manufacturing has been largely investigated during the last 20 years since the pioneering work of Yajima in 1975.<sup>1</sup> The fabrication of silicon carbide or silicon nitride fibres has received special attention.<sup>1–3</sup> However, despite the large number of studies on the conversion of polysilanes and polycarbosilanes into silicon carbide, there are still unresolved problems concerning the crystallisation of these materials.<sup>4,5</sup>

Crystallisation may degrade the mechanical properties of silicon carbide fibres by altering the original smooth surface as grains are developed; this process can eventually destroy the fibre-like

morphology. Some research work was thus developed to try to inhibit the crystallisation process and to shift it to higher temperatures<sup>6–8</sup> by incorporation of additional elements such as boron or nitrogen in the starting polymeric precursor. But this would be a very costly process in the case of boron or would affect the thermal stability of the ceramic material in the case of nitrogen. In the Yajima process, oxygen was originally used to crosslink the polycarbosilane fibres,<sup>1</sup> and its presence had a dramatic effect on the thermal stability of the derived fibres, even worse than the introduction of nitrogen, especially when excess carbon was present, which is quite common in a large number of polycarbosilane-derived silicon carbides.<sup>9,10</sup>

Another way to raise the application temperature is to control the crystallisation of the material produced. For this the crystallite size should be as small as possible, e.g. no more than a few nanometers. But in the case of silicon carbide, not just one single phase usually crystallises. Due to the existence of many polytypes, the crystallisation leads to the formation of different SiC phases. At lower temperatures around 1200°C the 3C polytype (cubic) crystallises preferentially. Transformation of this polytype into  $\alpha$ -types may occur at temperatures around 2000°C, but the formation of the  $\alpha$ -polytypes (hexagonal or rhombohedral) depends on thermodynamic conditions. Either these polytypes crystallise directly from the amorphous phase during the silicon carbide formation or they form out of the crystalline  $\beta$ -silicon carbide phase. The temperature range between 1500 and 2200°C is the typical temperature range for the formation of these  $\alpha$ -polytypes. The most commonly observed ones are the 6H, 4H and 15R types. But the differences in enthalpy of the various silicon carbide polytypes are not really significant and simultaneous formation of a variety of polytypes usually occurs.

The purpose of this paper is to investigate the crystallisation behaviour of a polymer-derived amorphous silicon carbide material by XRD, TEM,  $^{29}\text{Si}$  MAS-NMR and Raman spectroscopy. Knowledge about the crystallisation could help to control the high-temperature alteration of the material in order to improve the fibre properties.

The starting polymeric precursor is a chlorine-containing polysilane derived from a disilane fraction of Müller–Rochow synthesis. The synthesis of the polymer was performed by a catalytic redistribution that has already been described in the literature.<sup>11,12</sup> The composition of such polymers may vary in a certain range (especially the chlorine content). For the manufacture of silicon carbide, a C/Si molar ratio close to 1 is expected after pyrolysis. For this reason, polymers with typical composition  $\text{SiC}_{1.5}\text{H}_{3.6}\text{Cl}_{0.8}$  have been used. The  $^{29}\text{Si}$  NMR spectra show the presence of silane sites containing Si–Cl bonds such as terminal  $\text{MeCl}_2\text{Si}$ - or linear  $\text{MeClSi}$ - groups as well as tertiary silane sites,  $\text{MeSi}(\text{Si})_3$ . The polysilane network is highly crosslinked, and forms a polycyclic structure. A detailed description of such polymers is given in Ref. 11.

After pyrolysis at 800°C, an amorphous SiC structure is obtained. Its composition depends on the starting polymer, but contains typically 59 wt% Si, 35 wt% C, 2 wt% H and 4 wt% Cl and some oxygen (< 1 wt%). Some detailed investigations concerning the state of the carbon (amorphous, glassy graphitic or silicon-bonded) of these pyrolysis products were already published.<sup>13</sup>  $^{29}\text{Si}$  NMR spectra show a broad peak around –12 ppm characteristic of an amorphous SiC structure based on  $\text{SiC}_4$  sites. The XRD pattern is quite consistent with an amorphous structure.

## Experimental

As mentioned in the introduction the synthesis of the polymer has already been reported.<sup>11</sup> The main idea is a catalytic redistribution of disilanes to form oligomers and subsequently polysilanes.

The pyrolysis was performed at 10 K  $\text{min}^{-1}$  under argon flow of 5 litres  $\text{h}^{-1}$  in an alumina tube furnace or carbon heated high temperature furnace (for  $T > 1500^\circ\text{C}$ ). The maximum temperatures ranged from 1000°C to 1800°C with dwell times from a few minutes to 12 h.

XRD measurements were performed with TURM-62-HZG 4 (Carl Zeiss Jena) equipment using the  $\text{Co } K_\alpha$  radiation. The  $2\theta$  range was 25 to 60° and the step width was 0.1° each in 30 s.

Raman spectra were recorded with a GDM 1000 L apparatus equipped with an  $\text{Ar}^+$  ion laser

(514.5 nm line). The power was limited to 30 mW to avoid any alteration of the samples. The area of the laser beam was focused on a diameter of 100  $\mu\text{m}$  so that a characteristic volume of the sample was investigated.

TEM investigations were performed with a 100CX III JEOL equipment. Observations were performed on powders placed on a copper grid. A gold standard was used for calibration of the electron diffraction measurements.

$^{29}\text{Si}$  MAS-NMR spectra were recorded on a Bruker MSL 400 spectrometer (79.5 MHz). The spinning rate was 5 kHz. The pulsewidth was 2  $\mu\text{s}$  ( $\theta = 30^\circ$ ) and the recycle delay 60 s. Sixty transients were accumulated and 20 Hz linebroadening was applied before Fourier Transformation. The spectra were simulated with the WINFIT program.<sup>14</sup>

## Results

### X-ray diffraction

The X-ray diffraction patterns of samples between 1200 and 1800°C are shown in Fig. 1. Samples treated at temperatures lower than 1200°C show almost no X-ray peaks and can be considered as completely X-ray amorphous. The crystallisation is rather poor up to 1400°C. The broad X-ray peak centred around  $2\theta = 41.7^\circ$  should be attributed to the most intense peak of  $\beta$ -SiC

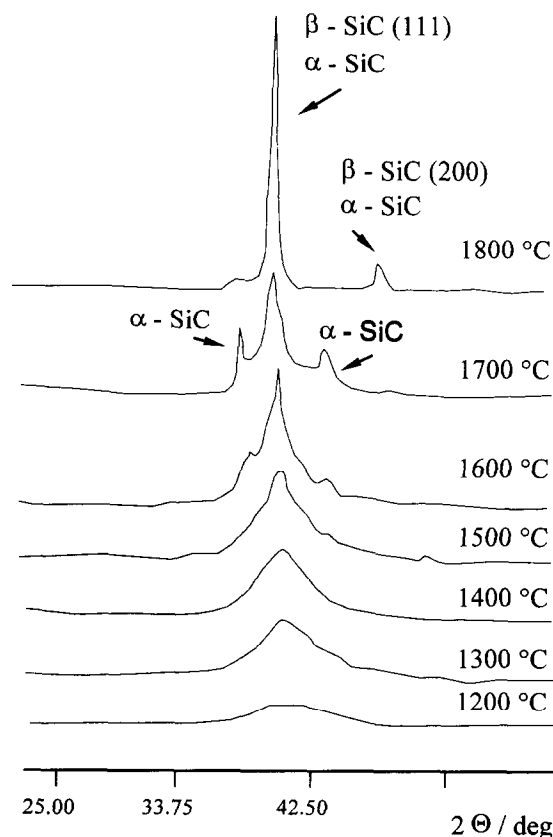


Fig. 1. X-ray diffraction patterns of pyrolysed polysilanes versus pyrolysis temperature.

corresponding to  $d = 2.51 \text{ \AA}$  (111). This peak is also found in the  $\alpha$ -polytypes (4H (004), 6H (102, 006), 15R (0.0.15)) but in this case other peaks should also be detected around  $2\theta = 39^\circ$  ( $d = 2.65 \text{ \AA}$ ) and  $45^\circ$  ( $d = 2.35 \text{ \AA}$ ) for 4H, 6H and 15R species.

Due to the broadness of the diffraction peaks the (200) peak that is characteristic of the 3C polytype and which should be present in the considered  $2\theta$  range (e.g.  $2\theta = 48.6^\circ$ ,  $d = 2.18 \text{ \AA}$ ), but with a lower intensity than the (111) peak (20%), was not detected. Crystallite growth directly related to the peak linewidth, is not significant at temperatures below  $1500^\circ\text{C}$ , even after long dwell times, but occurs significantly at  $1500^\circ\text{C}$ . Above this temperature, the X-ray peaks sharpen with increasing treatment temperatures and dwell time.

Crystallite growth is not the only phenomenon to occur. Additional changes in the polytype natures are observed. New peaks are present in the patterns of samples heat treated at  $T > 1500^\circ\text{C}$ . These additional peaks at about  $39^\circ$  and  $45^\circ$  ( $d = 2.65$  and  $2.35 \text{ \AA}$  respectively) are assigned to  $\alpha$ -polytypes as already mentioned. A significant amount of such polytypes is formed in the sample heat treated at  $1700^\circ\text{C}$ . However an exact identification of the different polytypes is rather uncertain based only on the X-ray patterns. Surprisingly, this change from  $\beta$ - into  $\alpha$ - silicon carbide seems to be completely suppressed when a temperature of  $1800^\circ\text{C}$  is reached, where only the (111) and the (200) peaks of  $\beta$ -SiC are detectable.

Figure 2 shows the evolution of the crystallite size calculated from Scherrer formula (dwell time 15 min) versus temperature. The (111) peak, which is first observed in the sample treated at  $1200^\circ\text{C}$ , gives a mean crystallite size around 1.5 nm. This value does not change very drastically up to  $1400^\circ\text{C}$  (2 nm). At  $1500^\circ\text{C}$  a mean crystallite size of 3 nm is reached which increases to 4 nm at

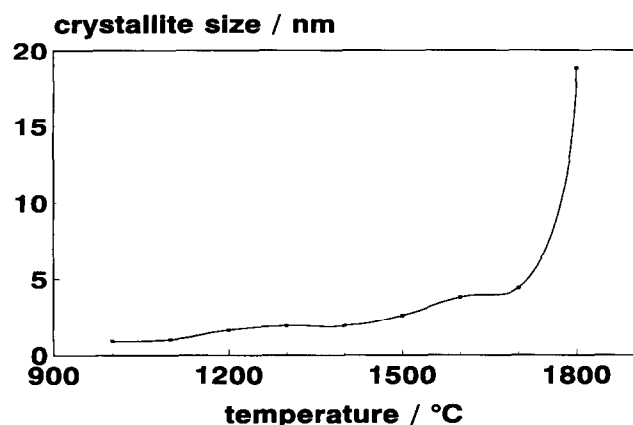


Fig. 2. Crystallite size of polysilane-derived silicon carbide versus temperature, calculated from peak width, dwell time 15 min at the quoted temperatures.

$1600^\circ\text{C}$  and 4.5 nm at  $1700^\circ\text{C}$ . A very drastic growth is then observed since a mean crystallite size of 19 nm is estimated at  $1800^\circ\text{C}$ . The temperature range between 1700 and  $1800^\circ\text{C}$  is obviously the range where the activation energy for crystallisation exceeds the level for growth and the former crystallite faults which prevent the crystallite growth can be cured by rearrangement of the atoms in the crystallite structure.

### Raman spectroscopy

The Raman spectra of the 1700 and  $1800^\circ\text{C}$  samples are shown in Fig. 3. The 3C polytype is characterised by a LO band at  $793 \text{ cm}^{-1}$  and a TO band at  $970 \text{ cm}^{-1}$ ,<sup>15</sup> while the 6H polytype should present bands at 791 and  $765 \text{ cm}^{-1}$ .<sup>15</sup> The spectrum of the  $1700^\circ\text{C}$  sample shows unambiguously the presence of the 3C and 6H polytypes while the spectrum of the  $1800^\circ\text{C}$  sample only gives evidence for the presence of pure 3C polytype with a unique band at  $793 \text{ cm}^{-1}$ . However the LO band of the 3C polytype expected at  $970 \text{ cm}^{-1}$  is no longer seen in the spectrum of the  $1800^\circ\text{C}$  sample. The reasons for that could be either very small crystallite sizes or coupling of the LO phonons with charged particles in the material. The TO phonons are not influenced by such effects. The first reason can be ruled out because the  $1800^\circ\text{C}$  sample presents much larger crystallite size than the  $1700^\circ\text{C}$  sample. But, the second one can be possible, considering the results of first electrical measurements that were performed on these materials.

### TEM investigations

Samples heat treated at 1400, 1600 and  $1800^\circ\text{C}$  for respectively 15 min, 1 h and 15 min were investigated by TEM.

Figure 4 shows an image of the  $1400^\circ\text{C}$  sample and the related diffraction pattern. This sample is characterised by a nanocrystalline structure with

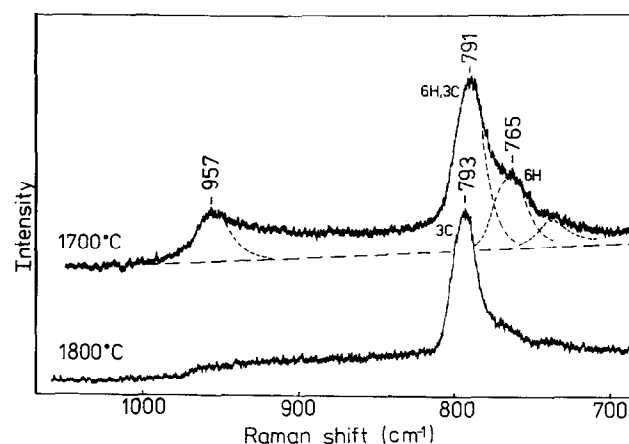
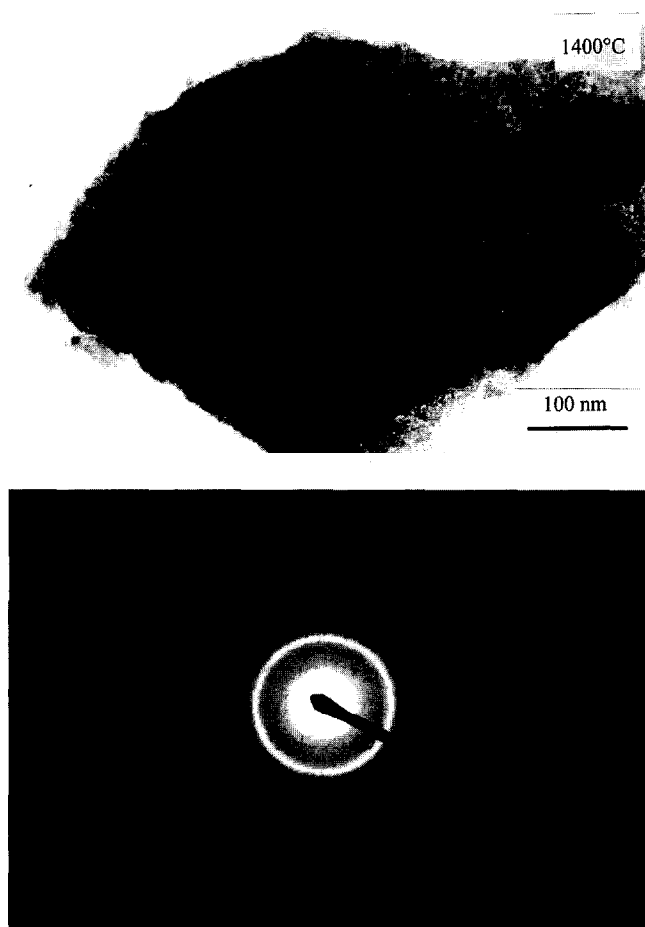


Fig. 3. Raman spectra of the 1700 and  $1800^\circ\text{C}$  samples, dwell time 15 min.



(a)

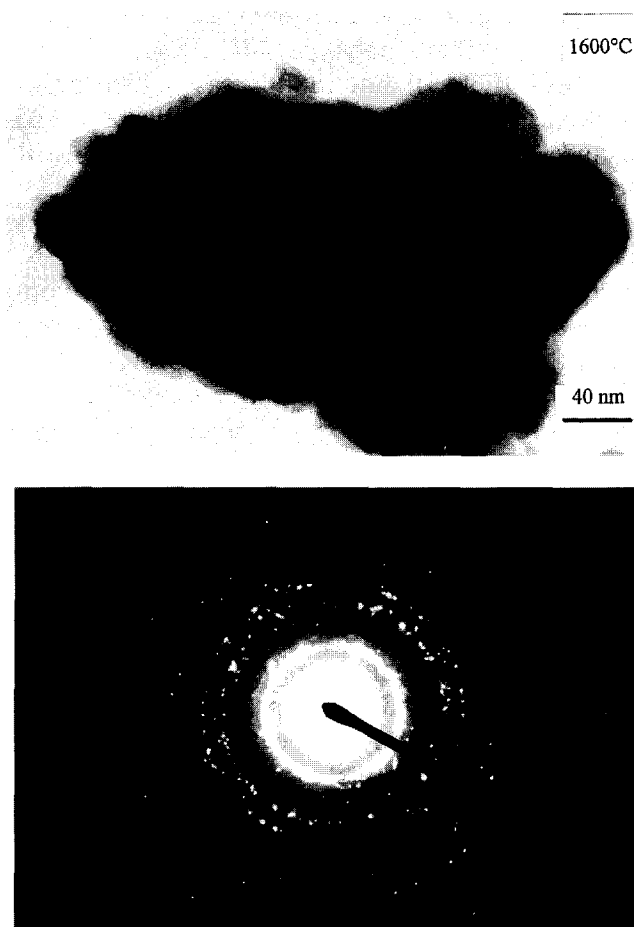
Fig. 4. TEM image and electron diffraction pattern (4(a)) of the 1400°C sample.

large areas of amorphous regions. The grain size, that can be estimated from the micrograph, is in the 2–5 nm range. Table 1 gives a comparison between the crystallite size values extracted from the X-ray and the grain size from the TEM measurements. They are in good agreement for this sample. The electron diffraction pattern shows that a long-range order already exists. The electron beam has diffracted on a large number of small crystallites, so that only rather diffuse diffraction rings are present, but they correspond only to  $\beta$ -SiC.

Figure 5 shows a typical TEM image of the 1600°C sample. A significant grain growth is observed compared to the 1400°C sample that should correspond with the crystallite size. This suggestion is evidenced by the more defined

Table 1. Comparison of crystallite and grain dimensions derived from X-ray diffraction and TEM observation

Sample	X-ray dimension crystallite size (nm)	TEM dimension grain size (nm)
1400°C, 1 h	2	3
1600°C, 1 h	4	45
1800°C, 1 h	19	119



(a)

Fig. 5. TEM image and electron diffraction pattern (5(a)) of the 1600°C sample.

electron diffraction pattern. The grains reach a size of about 50 nm (Table 1) but the crystallites do not enlarge their size in the same order (X-ray results). Probably the grains consist of a number of crystallites after this temperature. Moreover one can observe fringe systems which are characteristic for stacking faults or twins in the photograph as well as reflection splitting in the diffraction pattern. The polytypes detected by the electron diffraction patterns are  $\beta$ -SiC as well as  $\alpha$ -SiC. Obviously, the stacking faults already nucleate also  $\alpha$ -crystallites at these temperatures. The observed structure of the electron diffraction patterns additionally shows that a great number of crystal defects exist in the material. One finds well-defined points in the electron diffraction pattern. Some of these points are attributed to  $\alpha$ -SiC as for  $d = 2.31$  and  $2.58$  Å. This is in agreement with the X-ray results. But the electron diffraction pattern shows single streaked reflections which are obviously caused by planar defects.

The 1800°C sample shows larger crystals and sharper diffraction patterns (Fig. 6). But the crystal faults still exist which are detected by the micrograph as well as by the diffraction pattern.



Fig. 6. TEM image and electron diffraction pattern (6(a)) of the 1800°C sample.

The basic structure of the material is the 3C polytype as was found by other methods. Some angle shifted diffraction points are detected which obviously contributed to the discussed  $\alpha$ -polytypes (marked with an arrow). The reflections of the cubic phase form streaks which are caused by twinning or stacking faults. But only few points are in the pattern so that now only a single crystal is examined. The difference between the crystallite size calculated from the X-ray peak broadening and grain size observed by the TEM micrograph is enormous. The commonly observed grain size is about 100 nm by TEM with a crystallite size of 19 nm by X-ray broadening. This means that the number of the observed stacking faults drastically limits the area of the coherent crystallite size.

### <sup>29</sup>Si MAS-NMR

Figure 7 shows the <sup>29</sup>Si MAS-NMR spectra recorded on selected pyrolysed samples. The signals of the samples which were pyrolysed at 1400°C or 1500°C show clearly two components, one around -15/-16 ppm and the other around -19/-20 ppm, with a third component as a shoulder more or less well defined around -25 ppm. The

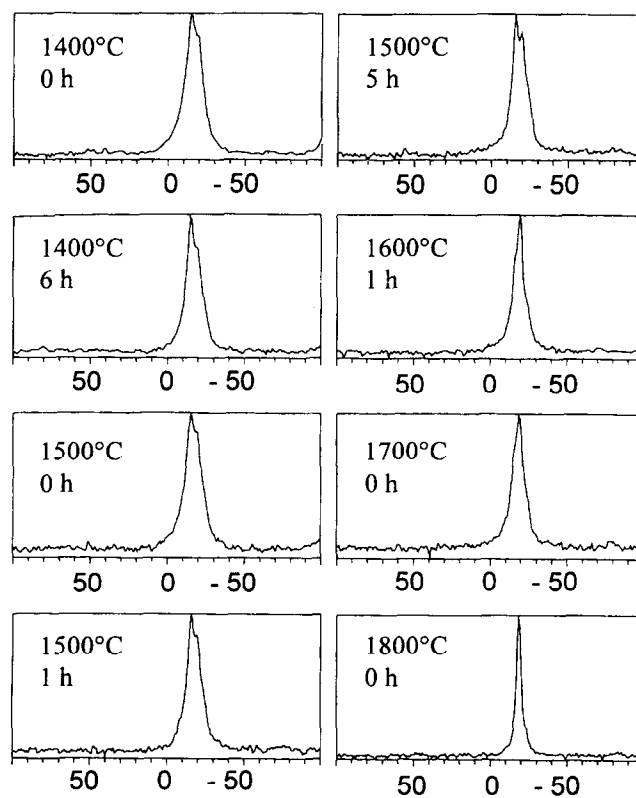


Fig. 7. <sup>29</sup>Si MAS-NMR spectra of pyrolysed polysilane samples.

spectra of the samples fired at 1600°C and 1700°C seem to present the same components, but with an increase of the signal around -19 ppm. As for the 1800°C sample, the signal is much sharper, centred around -19 ppm.

In order to extract the various components, the spectra have been simulated and the results are reported in Table 2. Three components (P1, P2 and P3) have been introduced. The chemical shift values correspond to values found for SiC polytypes.<sup>16-21</sup> Figure 8 demonstrates the fitting procedure for the 1700 and 1800°C samples. Table 3 summarises some <sup>29</sup>Si NMR data collected in the literature on various SiC polytypes. Hartman *et al.*<sup>19</sup> found four possible types of Si surroundings in SiC polytypes which they called A<sup>Si</sup>, B<sup>Si</sup>, C<sup>Si</sup> and D<sup>Si</sup>; all the chemical shift values for the different sites are very close. Moreover, in the case of the cubic polytype 3C, where only one site is expected, different values of chemical shift have been published depending on the nature of the sample (powder, single crystal, whiskers). An excellent paper from Carduner *et al.*<sup>21</sup> clearly showed the importance of stacking faults in  $\beta$ -SiC samples: they examined different commercial  $\beta$ -SiC powders and found that the <sup>29</sup>Si NMR response could be either a narrow peak around -16 ppm, accompanied by some minor features due to structure units of  $\alpha$ -phases, or a broader signal centred at -18/-19 ppm. They concluded that these differences came from the formation of

**Table 2.** Results from the simulations of the  $^{29}\text{Si}$  MAS-NMR spectra of pyrolysed samples

Samples	Peak label	Chemical shift (ppm)	Linewidth (ppm)	Percentage
1400°C, 15 min	P2	-20.4	6.6	25
	P1	-14.7	9.7	75
1400°C, 6 h	P3	-23.9	3.9	10
	P2	-20.0	4.4	21
	P1	-15.1	6.9	69
1500°C, 15 min	P3	-24.1	4.3	7
	P2	-20.1	4.6	18
	P1	-15.1	8.9	75
1500°C, 1 h	P3	-24.0	5.3	15
	P2	-20.0	3.9	21
	P1	-15.8	6.4	64
1500°C, 5 h	P3	-24.2	3.9	13
	P2	-20.1	4.1	31
	P1	-15.5	5.4	56
1600°C, 1 h	P3	-24.4	4.7	10
	P2	-19.3	4.6	47
	P1	-16.3	7.1	43
1700°C, 15 min	P3	-24.5	3.2	7
	P2	-19.7	4.9	49
	P1	-16.0	6.6	44
1800°C, 15 min	P3	-23.0	2.5	3
	P2	-18.7	3.6	97

stacking disorders in the SiC particles. A sharper resonance should be related to an ordered  $\beta$ -phase as predominant component, while a broader peak should be related to a disordered structure. All

these studies show clearly that the assignments of the resonance peaks to precise Si sites is far from obvious in such systems.

At 1400°C and 1500°C, the main component is the P1 (-15 ppm) resonance peak whose position is slightly shifted upfield by increasing the firing temperature and/or by increasing the time of heat treatment. An upfield shift has already been reported in the literature for the conversion of the Yajima polycarbosilane into SiC<sup>9</sup> and assigned to deprotonation reactions occurring at the C sites and causing a change in the chemical shift of the Si sites. In the present case, the same explanation can be given even if, at such temperature, the number of C-H bonds should be very small. The shift can also be related to an ordering of the various sites. This peak can be assigned to the presence of sites C<sup>Si</sup> from  $\beta$ -SiC phases considering its chemical shift value and its intensity. If it were due to sites A<sup>Si</sup> from an  $\alpha$ -phase, other peaks would be expected, due to sites B<sup>Si</sup> and C<sup>Si</sup>, of equal intensity.

The peak P2 is more difficult to assign, because its chemical shift value is in a range where contributions from various polytypes can overlap. It is interesting to point out that its intensity increases with the heat treatment time, while the intensity of the P1 peak decreases. This tendency is even more pronounced at higher temperatures, 1600°C and 1700°C, where this signal becomes dominant. Finally, at 1800°C, it seems that only this peak at -18.7 ppm now remains. The XRD pattern of the

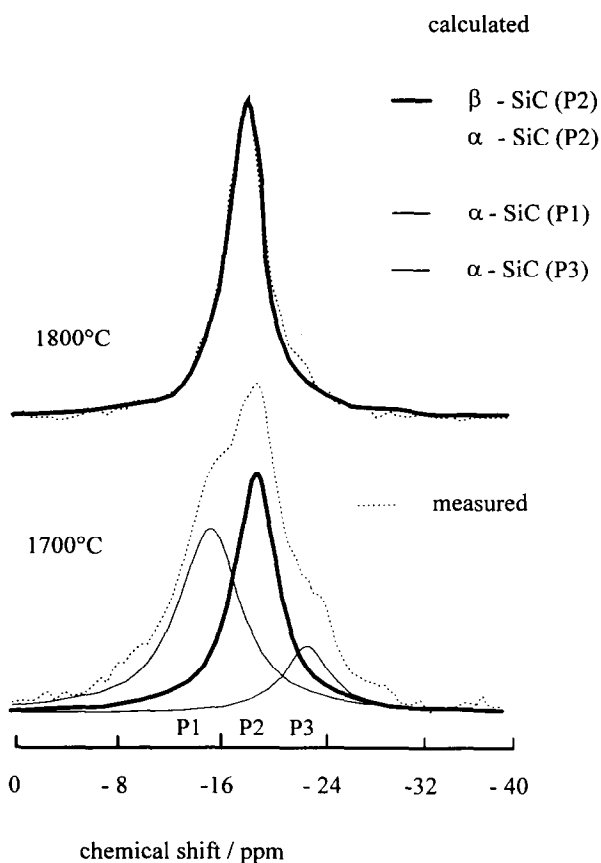


**Fig. 8.** Example for the deconvolution of the obtained  $^{29}\text{Si}$  MAS-NMR spectra of the 1700 and 1800°C samples.

**Table 3.**  $^{29}\text{Si}$  chemical shifts for various SiC polytypes extracted from literature

Samples	Site (Intensity ratio)	Chemical shift (ppm)	Reference
$\beta$ -SiC (3C) crystals crystal powder crushed bulk whiskers	C	-18.3	18
		-16.1	16
		-18.4	16
		-17.2	17
		-20	17
$\alpha$ -SiC (6H)	A B C (1/1/1)	-13.9; -20.2; -24.5	18,19
		-14.3; -20.4; -24.9	16
$\alpha$ -SiC (15R)	A B C (1/2/2)	-14.9; -20.8; -24.4	19
		-14.6; -20.5; -24.1	16
$\alpha$ -SiC (2H)	D	-20.0	20
$\alpha$ -SiC (4H)	B C (1/1)	-19.7; -22.5	20

1800°C sample is characteristic of  $\beta$ -SiC with some traces of  $\alpha$ -phase: it seems thus correct to assign peak P2 to Si sites in crystalline  $\beta$ -SiC phase. The small P3 peak at -23 ppm could be due to sites C<sup>Si</sup> of polytype 6H in agreement with the XRD and Raman spectra.

It thus seems that the two peaks P1 and P2 could be assigned to Si sites of the  $\beta$ -polytypes. By reference to the paper from Carduner *et al.*<sup>21</sup> the chemical shift values for P1 could correspond to ordered SiC crystallites, while the peak P2 could be due to disordered SiC phase with stacking faults.

The peak P3 is present in all the spectra and shows the presence of Si sites of type C<sup>Si</sup> only present in  $\alpha$ -polytypes such as 4H, 6H or 15R. Its intensity seems to increase with the heat treatment time at 1500°C, but never exceeds 15% of the total amount of Si sites. The presence of some  $\alpha$ -polytypes is in agreement with the XRD and electron diffraction results.

A continuous sharpening of the various peaks either by increasing the firing temperature or the firing time can also be seen. This can be related to an ordering of the various Si sites in a more crystalline structure.

## Discussion

From the above results some conclusions can be drawn concerning the crystallisation behaviour of these polymer-derived silicon carbide samples.

The amorphous SiC structure starts to crystallise around 1200°C. Very small crystallites of  $\beta$ -SiC, less than 2 nm in size, are observed at this temperature and no crystallite growth is detected even after long treatment time (12 h). The amor-

phous part of the material still contains a certain amount of hydrogen and chlorine, and is characterised by a signal between -14 and -16 ppm in the corresponding  $^{29}\text{Si}$  MAS-NMR spectra. This peak P1 (Table 2) becomes weaker with higher temperature and longer dwell time. However, even at 1400°C the carbon atoms are partly hydrogenated and the material still contains about 2 wt% chlorine. At that temperature a moderate growth of the  $\beta$ -SiC crystallites starts that is associated with the formation of numerous stacking faults which will nucleate also crystallites of  $\alpha$ -polytype in the samples. These  $\alpha$ -silicon carbide polytype areas are observed by X-ray diffraction as well as by Raman spectroscopy and electron diffraction. The NMR spectra present two major signals (P1 and P2) indicating the presence of ordered and disordered  $\beta$ -SiC phases, but also a peak at -23 ppm (P3) that shows unambiguously the presence of Si sites characteristic of structure units of  $\alpha$ -polytypes. This peak was found in almost all samples except for the 1400°C (15 min) sample. The formation of  $\alpha$ -SiC is caused by the creation of stacking faults that act as nuclei for these instable polytypes during the preferred  $\beta$ -SiC crystallisation. The insufficient mobility of the atoms at temperatures lower than 1600°C does not enable rearrangement of the formed  $\alpha$ -SiC-crystal regions into a  $\beta$ -SiC crystals or at least affects it drastically. The NMR spectra of samples heat treated at  $T > 1600^\circ\text{C}$  show a decreasing intensity for the P3 peak. However, this observation seems in disagreement with the XRD results of the 1600 and 1700°C samples, for which more significant peaks due to the 6H polytype are observed. But this difference between the two techniques may be caused by the change in the amount of amorphous phases in the samples. The P3 signal is certainly caused by stacking faults in the crystals or similar local structures in the amorphous material. These local  $\alpha$ -like structures are not detected in the X-ray pattern but they are observed in the NMR spectra. Probably the nanocrystalline regions are the first which are rearranged into more  $\beta$ -silicon carbide-like structures, so that the intensity of the P3 NMR signal decreases. This does not affect the X-ray pattern where more defined SiC crystals become detectable and show clearly separated polytype signals.

The crystallisation process is completed at 1800°C when almost pure  $\beta$ -silicon carbide is found by all investigation methods. Large grains of about 100 nm and crystallites of 20 nm exist. The rapid crystallite growth is obviously enabled by the higher mobility of the atoms that leads partly to a rearrangement of the  $\alpha$ -like structures and stacking faults in the already existing  $\beta$ -SiC

crystals which are drastically expanded after that temperature. In this way the unexpected transformation of the  $\alpha$ -SiC into  $\beta$ -SiC becomes understandable when the usual option of a strong impediment of the  $\alpha \rightarrow \beta$  transformation is regarded as valid on a global level but, obviously in the investigated case, it is on a local scale that transformation occurs.

### Acknowledgements

We are grateful to the Deutsche Forschungsgemeinschaft and the Deutscher Akademischer Austauschdienst for financial support of the collaboration between the University P. et M. Curie, Paris and the Freiberg University. We would like more specifically to thank Prof. G. Roewer and his coworkers (Department of Inorganic Chemistry, Freiberg University), who provided the polysilanes, for helpful discussions and advice. Mr M. Lavergne (Centre de Microscopie, University P. et M. Curie) is also greatly acknowledged for the TEM investigations.

### References

1. Yajima, S., Continuous SiC-fibres of high tensile strength. *Chem. Letters*, **9** (1975) 931–934.
2. Takeda, M., Imai, Y., Ishikawa, H., Ishikawa, T., Seguchi, T. & Okamura, K., Thermal stability of the low oxygen silicon carbide fibres derived from PCS. *Ceram. Eng. Sci. Proc.*, **(12)**[7–8] (1992) 209–217.
3. Mocaer, D., Pailler, R., Naslain, R., Richard, C. *et al.*, Si–C–N ceramics with high microstructural stability elaborated from the pyrolysis of new polycarbosilane precursors, Part I: The organic/inorganic transition. *J. Mat. Sci.*, **28** (1993) 2615–2631.
4. Lippowitz, J., Freeman, H. A., Chen, R. T. & Prack, E. R., Composition and structure of ceramic fibers prepared from polymer precursors. *Adv. Ceram. Mat.*, **2** (1987) 121–128.
5. Yokoyama, Y., Nanba, T., Yasui, I., Kaya, H., Maeshima, T. & Isoda, T., X-ray diffraction study of the structure of silicon nitride fiber made from perhydropolysilazane. *J. Amer. Ceram. Soc.*, **74** (1991) 654–657.
6. Riedel, R., Kienzle, A., Szabó, V. & Mayer, J., Hydroboration of polymethylvinylsilane — a novel route to silicon boron carbide ceramics. *J. Mat. Sci.*, **28** (1993) 3931–3938.
7. Mocaer, D., Pailler, R., Naslain, R., Richard, C. *et al.*, Si–C–N ceramics with high microstructural stability elaborated from the pyrolysis of new polycarbosilane precursors, Part IV: Oxygen-free model monofilaments. *J. Mat. Sci.*, **28** (1993) 3049–3058.
8. Funayama, O., Nakahara, H., Tezuka, A., Ishii, T. & Isoda, T., Development of Si–B–O–N fibres from polyborosilazane. *J. Mat. Sci.*, **29** (1994) 2238–2244.
9. Soraru, G. D., Babonneau, F. & Mackenzie, J. D., Structural concepts on new amorphous covalent solids. *J. Non-Crystal. Solids*, **106** (1988) 256–261.
10. Bouillon, E., Mocaer, D., Villeneuve, J. F., Pailler, R. & Naslain, R., Conversion mechanisms of a polycarbosilane precursor into a SiC-based ceramic material. *J. Mat. Sci.*, **26** (1991) 1517–1530.
11. Richter, R., Roewer, G., Böhme, U. *et al.*, Reactive silicon organic polymers — new aspects on synthesis of silicon carbide precursors. *Appl. Organomet. Chem.* (1996) in press.
12. Babonneau, F., Richter, R., Bonhomme, C., Maquet, J. & Roewer, G., NMR investigations of the polysilane–polycarbosilane transformation of poly(methylchlorosilanes). *J. Chim. Phys.*, **92** (1995) 1745–1748.
13. Martin, H.-P., Irmer, G., Schuster, G. & Müller, E., Structural investigations on pyrolysed polysilanes. *Fres. J. Anal. Chem.*, **349** (1994) 160–161.
14. Massiot, D., Thiele, H. & Germanus, A., Bruker Report, 1994, 140, 43.
15. Dando, N. R. & Tadayyoni, M. A., Characterisation of polyphasic silicon carbide using surface enhanced Raman and nuclear magnetic resonance spectroscopy. *J. Am. Ceram. Soc.*, **73** (1990) 2242.
16. Guth, J. R. & Petuskey, W. T., Silicon-29 magic angle spinning nuclear magnetic resonance characterisation of SiC polytypes. *J. Phys. Chem.*, **91** (1987) 5361.
17. Wagner, G. W., Na, Byung-Ki & Vanice, A., High resolution solid state NMR of  $^{29}\text{Si}$  and  $^{13}\text{C}$  in  $\beta$ -silicon carbide. *J. Phys. Chem.*, **93** (1989) 5061.
18. Finlay, G. R., Hartman, J. S., Richardson, M. F. & Williams, B. L.,  $^{29}\text{Si}$  and  $^{13}\text{C}$  magic angle spinning NMR spectra of silicon carbide polymorphs. *J. Chem. Soc., Chem. Commun.* (1985) 159.
19. Hartman, J. S., Richardson, M. F., Sherriff, B. L. & Winsborrow, B. G., Magic angle spinning NMR studies of silicon carbide polytypes, impurities and highly inefficient spin-lattice relaxation. *J. Am. Chem. Soc.*, **109** (1987) 6059.
20. Apperley, D. C., Harris, R. K., Marshall, G. L. & Thompson, D. P., Nuclear magnetic resonance studies of silicon carbide polytypes. *J. Am. Ceram. Soc.* **74** (1991) 777.
21. Carduner, K. C., Shinozaki, S. S., Rokosz, M. J., Peters, C. R. & Whalen, T. J., Characterisation of  $\beta$ -silicon carbide by silicon -29 solid-state NMR, Transmission Electron Microscopy and Powder X-ray Diffraction. *J. Am. Ceram. Soc.*, **73** (1990) 2281–2286.